RESEARCH ARTICLE OPEN ACCESS

Experimental study of the effect of baffle types on the performance of a shell and tube heat exchanger

Abdullah Atif Bakheet[1], Majed Alhazmy[1], and El-Sayed R. Negeed[1,2].
[1]*Faculty of Engineering, Department of Mechanical Engineering, Jeddah, King Abdulaziz University, P.O. Box 80204, Jeddah, 21589, Saudi Arabia.*
[2]*Reactors Department, Nuclear Research Center, Atomic Energy Authority, P.O. Box 13759, Cairo, Egypt.*

ABSTRACT
This study experimentally investigated the effect of single-, double-, and triple-segmental baffle configurations on the thermal-hydraulic performance of a shell-and-tube heat exchanger. Experiments were conducted using water as the working fluid at shell-side flow rates of 10–25 L/min and tube-side inlet temperatures of 65, 70, and 75°C. Thermal performance was evaluated using the Nusselt number, number of transfer units (NTU), and effectiveness, while hydraulic performance was assessed through pressure drop, pumping power, and the Performance Evaluation Criterion (PEC). Statistical analyses, including two-way ANOVA and Tukey's HSD test, were performed to assess the significance of the observed differences. The triple-segmental baffle provided the best overall performance, increasing the average tube-side Nusselt number, NTU, and effectiveness by 24.31%, 16.43%, and 10.95%, respectively, while reducing pressure drop and pumping power by 28.21% and 24.9% compared with the single-segmental baffle. Statistical analysis confirmed significant effects of baffle configuration on the tube-side Nusselt number, NTU, and pressure drop ($p < 0.05$). The highest PEC value (1.128) was obtained with the triple-segmental baffle, demonstrating the most favourable balance between heat transfer enhancement and hydraulic performance.

Keywords: Shell-and-tube heat exchanger; Segmental baffles; Thermal-hydraulic performance; Nusselt number; Pressure drop; Performance Evaluation Criterion.

Date of Submission: 11-08-2026 Date of acceptance: 23-08-2026

I. Introduction

Heat exchangers are essential thermal devices used to transfer heat between two or more fluids at different temperatures without direct mixing [1]. Owing to their high reliability, mechanical robustness, and capability to operate over a wide range of pressures and temperatures, shell-and-tube heat exchangers (STHEs) remain the most widely used heat exchangers in power generation, petrochemical processing, oil and gas production, refrigeration, desalination, food processing, and chemical industries. Their widespread industrial application has motivated continuous efforts to improve heat transfer efficiency while simultaneously minimizing hydraulic losses and operating costs [2], [3].

The thermal performance of a shell-and-tube heat exchanger is governed primarily by the flow characteristics on the shell side. Baffles are incorporated to support the tube bundle, suppress flow-induced vibration, and redirect shell-side fluid across the tubes, thereby increasing turbulence and improving convective heat transfer. However, increasing turbulence generally increases pressure drop, resulting in higher pumping power requirements [4], [5]. Therefore, the design of baffle geometry represents a fundamental thermal-hydraulic optimization problem in which heat transfer enhancement must be balanced against hydraulic resistance.

Among the various baffle designs, segmental baffles remain the most commonly adopted because of their simple construction and effective promotion of shell-side crossflow [6]. Conventional single-segmental baffles generally provide high heat-transfer coefficients but often produce relatively large pressure drops because of repeated changes in flow direction. To overcome this limitation, alternative configurations such as double-, triple-segmental, helical, and other advanced baffle arrangements have been proposed to improve flow distribution, reduce dead zones, and decrease hydraulic resistance while maintaining acceptable heat-transfer performance [3], [7].

Recent investigations have demonstrated that optimizing baffle geometry can significantly improve the overall thermal-hydraulic performance of shell-and-tube heat exchangers. [5] reported that an optimized baffle configuration achieved an improved thermohydraulic performance by enhancing heat transfer while reducing pressure-drop penalties. Similarly, [2] emphasized that appropriate baffle geometry improves turbulence generation and flow distribution, leading to higher heat-transfer efficiency with acceptable hydraulic losses. Recent numerical investigations have also shown that modifications in baffle geometry and spacing substantially influence shell-side velocity distribution, pressure drop, and overall exchanger performance [3].

Although numerous numerical and computational fluid dynamics (CFD) studies have investigated different baffle configurations, comparatively fewer experimental studies have directly compared single-, double-, and triple-segmental baffles under identical operating conditions [3], [7]. Furthermore, many existing investigations primarily evaluate thermal performance using conventional parameters such as the Nusselt number, overall heat-transfer coefficient, or pressure drop, while comprehensive thermal-hydraulic assessment using statistical validation and integrated performance indicators remains limited [8], [9], [10]. As a result, the relative advantages of different segmental baffle configurations have not yet been fully quantified through experimental investigation.

Therefore, this study experimentally investigates the influence of single-, double-, and triple-segmental baffles on the thermal-hydraulic performance of a shell-and-tube heat exchanger. Experiments were conducted under identical operating conditions using different shell-side flow rates and inlet temperatures. The performance of each configuration was evaluated using the shell-side and tube-side Nusselt numbers, number of transfer units (NTU), effectiveness, pressure drop, pumping power, and the Performance Evaluation Criterion (PEC). In addition, descriptive statistics, percentage improvement analysis, two-way analysis of variance (ANOVA), and Tukey's honestly significant difference (HSD) test were employed to determine the statistical significance of the observed performance differences. The findings provide a comprehensive experimental assessment of the trade-off between heat-transfer enhancement and hydraulic losses, offering practical guidance for selecting suitable baffle configurations in industrial shell-and-tube heat exchanger applications.

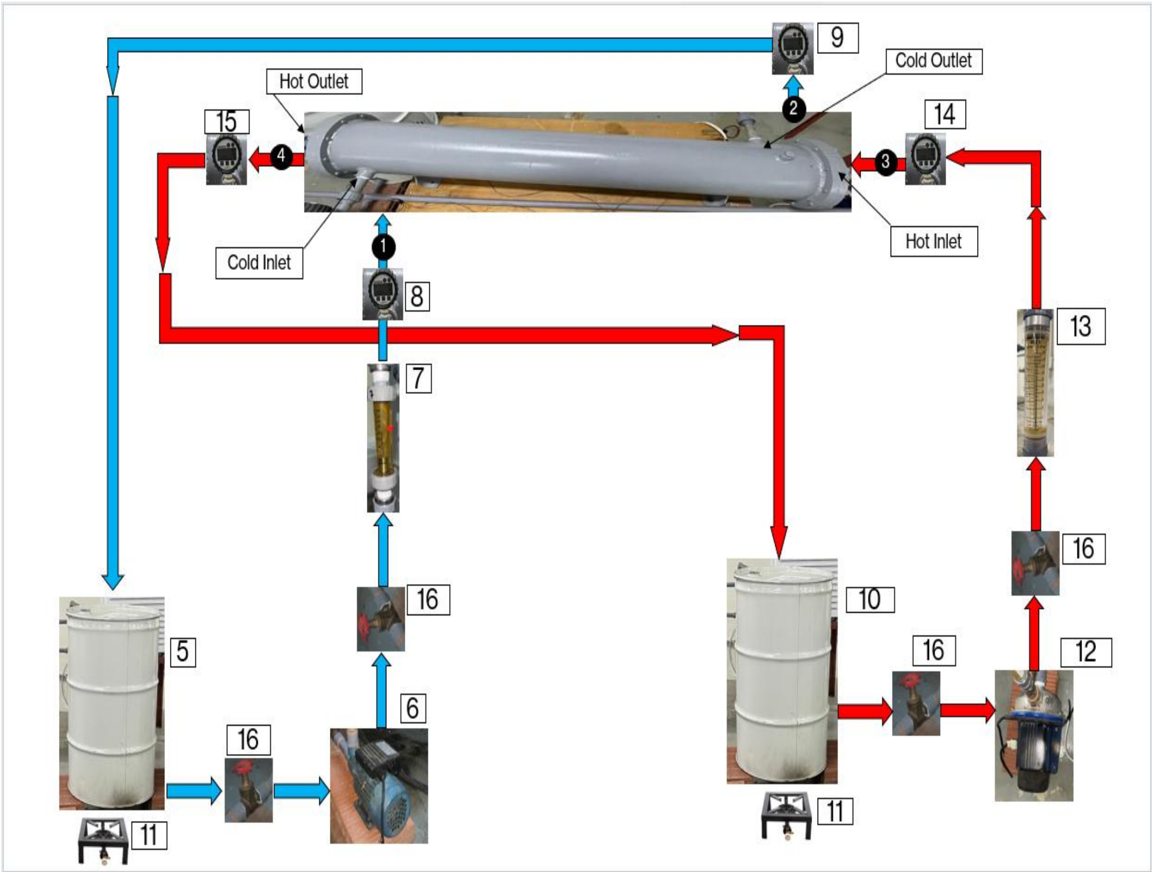

Figure 1. Schematic diagram of the experimental setup

Notes: (1) Thermocouple at the cold inlet (Shell side), (2) Thermocouple at the cold outlet (Shell side), (3) Thermocouple at the hot inlet (Tube side), (4) Cold water tank, (5) Cold water pump, (6) Flowmeter of cold water , (7) Flowmeter of cold water, (8) Pressure gauge of inlet cold water, (9) Pressure gauge of outlet cold water, (10) Hot water tank, (11) Hot water tank, (12) Hot water pump, (13) Flowmeter of hot water, (14) Pressure gauge of inlet hot water, (15) Pressure gauge of outlet hot water, (16) Gate valves.

II. Experimental Setup, Procedure, and Data Analysis

At the start of each experiment, the cold-water tank and the hot water tank are filled. Then, the heater and burner are switched on to heat the hot water to the required temperature for each experiment. The water temperature is measured using a Fluke meter to ensure it has reached the required temperature.

Next, the flow meter is set to the required flow rates for each experiment, and the Fluke meter is switched on to begin recording the temperature readings. The valves are then opened, allowing water to enter the heat exchanger. The cold-water flows into the shell side, and the hot water flows into the tube side.

The temperature readings are recorded by the Fluke meter, and the pressure is measured at both the shell side and tube side during the inlet and outlet phases of the experiment. This process continues for 30 minutes, the designated time for each experiment. Once the time is specified for each experiment, the valves are closed, the motors are switched off, and the experiment is complete. Finally, the water in the tube side is heated again to the required temperature, and the flow meters for both the hot and cold water are adjusted according to the required flow rates. These steps are repeated until all experiments are completed.

2.1. Evaluation of the Thermal and Physical Properties of Water

Water was used as the working fluid in both the shell side and tube side throughout all experiments. To ensure the accuracy of the thermal and hydraulic calculations, the thermal and physical properties of the water were evaluated, including density ρ, dynamic viscosity μ, thermal conductivity k, specific heat C_p, and Prantl number P_r.

The values of these properties were determined at the bulk temperature T_b for each experiment after stabilization. This bulk temperature was calculated based on the average of the fluid's inlet and outlet temperatures for both sides, where the bulk temperature represents the actual state of the fluid during heat transfer within the heat exchanger, according to the relationship, in [11]:

$$T_b = \frac{T_i + T_o}{2}, \tag{1}$$

2.2. Thermophysical properties of shell side can be determined:

Heat transfer coefficient h_0, can be determined, Fraas and P. [11]:

$$\frac{h_0 D_e}{k} = 0.36\,(\frac{D_e G_s}{\mu})^{0.55}(\frac{C_{pc}\mu}{k})^{\frac{1}{3}}(\frac{\mu}{\mu_w})^{0.14} \tag{2}$$

The wall temperature T_w was calculated using the methodology in [11]. The wall viscosity μ_w, was then determined at the wall temperature to ensure the accuracy of the wall viscosity correction in the Nusselt number equations, according to the relationship:

$$T_w = \frac{1}{2}\left(\frac{T_{h.i} + T_{h,o}}{2} + \frac{T_{c,i} + T_{c,o}}{2}\right) \tag{3}$$

The heat transfer rate Q_c in the shell, can be determined, [12]:

$$Q_c = \dot{m}_c\, C_{pc}\, \Delta T \;\;, \Delta T = \left(T_{c,i} - T_{c,o}\right) \tag{4}$$

Equivalent diameter D_e for a square pitch can be determined [11]:

$$D_e = \frac{4\,(P_T^2 - \pi\frac{d_0^2}{4})}{\pi\, d_0} \tag{5}$$

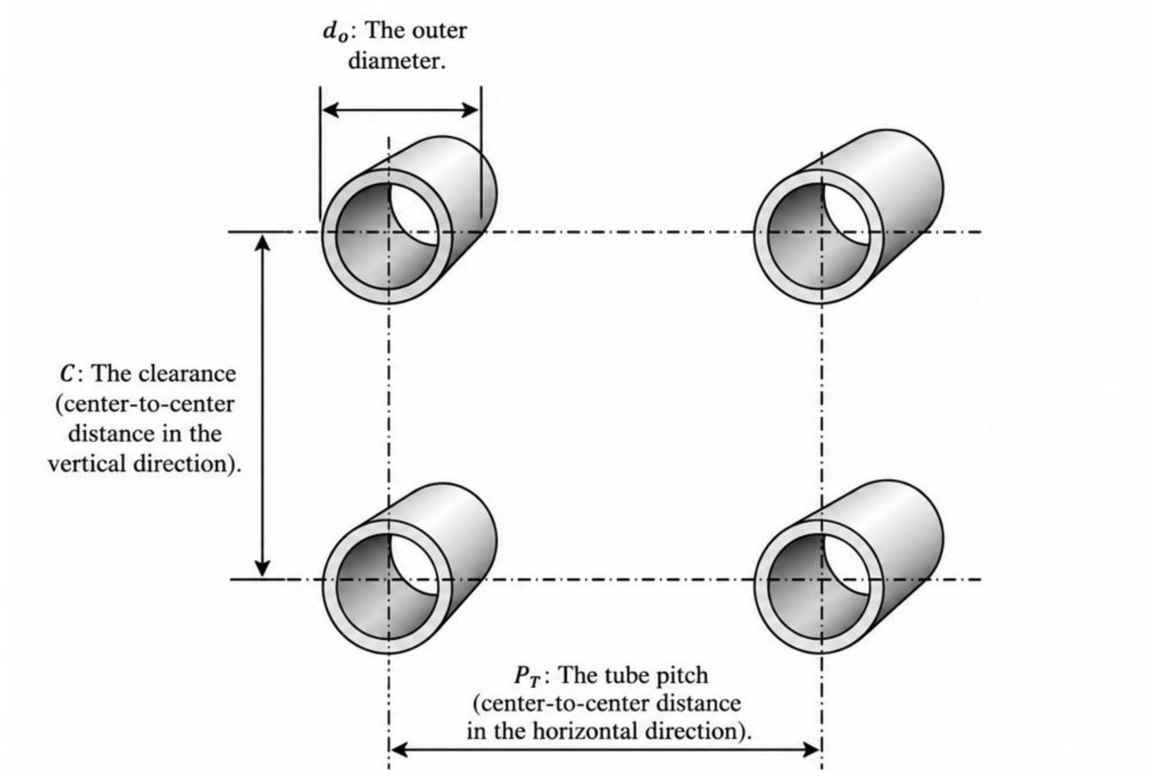

Figure 1 Square pitch tube layouts.

Where: d_o is the outer diameter of the tube (m), P_T is the tube pitch (center-to-center distance between adjacent tubes in the horizontal direction) (m), and C is the clearance (center-to-center distance between adjacent tubes in the vertical direction) (m).

The clearance C , can be determined:

$$C = P_T - d_0 \tag{6}$$

The bundle crossflow area A_s, at the center of the shell can be determined:

$$A_s = \frac{D_s\, C\, B}{P_T} \tag{7}$$

Shell-side mass velocity G_s, can be determined:

$$G_s = \frac{\dot{m}_c}{A_s} \tag{8}$$

Reynolds number Re_s, can be determined:

$$Re_s = \frac{D_e G_s}{\mu} \tag{9}$$

Prantl Number P_r, can be determined:

$$P_r = \frac{C_p \mu}{k} \tag{10}$$

2.3. Thermophysical properties of tube side can be determined:

The total area of tube A_{tp}, can be determined:

$$A_{tp} = \frac{\pi\, d_i^2}{4} \times N_t \tag{11}$$

The tube velocity u_m, can be determined:

$$u_m = \frac{\dot{m}_t}{\rho_t\, A_{tp}} \tag{12}$$

Reynolds number Re_t of the tube side, can be determined:

$$Re_t = \frac{\rho_t\, u_m\, d_i}{\mu} \tag{13}$$

The Nusselt number Nu, of turbulent in inner tube can be determined:

$$Nu = \frac{\left(\frac{f}{2}\right)(Re - 1000)\,Pr}{1.00 + 12.7\,(f/2)^{\frac{1}{2}}(pr_b^{\frac{2}{3}} - 1)}\ ,\ 2300 < Re < 10000 \qquad (14)$$

$$Nu = \frac{\left(\frac{f}{2}\right)(Re)\,Pr}{1.07 + 12.7\,(f/2)^{\frac{1}{2}}(pr_b^{\frac{2}{3}} - 1)}\ ,\ Re > 10000 \qquad (15)$$

$$f = (1.58 \ln Re - 3.28\,)^{-2} \qquad (16)$$

The heat transfer rate Q_h, in the tube, can be determined, [12]:

$$Q_h = \dot{m}_h\, C_{ph}\, \Delta T\ \ , \Delta T = \left(\,T_{h,o} - T_{h,i}\,\right) \qquad (17)$$

So, the heat transfer rate average, Q_{avg}, can be determined,

$$Q_{avg} = \frac{Q_h + Q_c}{2} \qquad (17)$$

The logarithmic mean temperature difference ΔT_{LM}, can be determined:

$$\Delta T_{LM} = \frac{\Delta T_1 - \Delta T_2}{\ln(\frac{\Delta T_1}{\Delta T_2})} \qquad (18)$$

Where:
$\Delta T_1 = T_{h,i} - T_{c,o}$
$\Delta T_2 = T_{h,o} - T_{c,i}$
The number of transfer units (NUT) in the tube can be estimate:

$$NUT = \frac{U_i A_i}{C_{min}} = \frac{Q_{avg}}{C_{min}\,\Delta T_{LM}} \qquad (19)$$

Where:
$A_i = N_t\, \pi\, d_i\, L$
C_{min}: The minimum value of C_c *and* C_h
$C_c = \dot{m}_c\, C_{p_c}$
$C_h = \dot{m}_h\, C_{p_h}$
The effectiveness in the tube ε, can be determined:

$$\varepsilon = \frac{Q_{actual}}{Q_{max}} = \frac{1 - \exp[-NUT(1 - cr)]}{1 - cr\,\exp[-NUT(1 - cr)]} \qquad (20)$$

Where:
$C_r = \frac{C_{min}}{C_{max}}$
$Q_{max} = C_{min}\,\Delta T_{max}$
$\Delta T_{max} = T_{h,i} - T_{c,i}$
The overall heat transfer coefficient with considering fouling U_f, can be determined:

$$U_f = \frac{1}{\frac{d_o}{d_i\,h_i} + \frac{d_o\,R_{f_i}}{d_i} + \frac{d_o \ln(d_o/d_i)}{2\,K} + R_{f_o} + \frac{1}{h_o}} \qquad (21)$$

The overall heat transfer coefficient without fouling U_f, can be determined:

$$U_f = \frac{1}{\frac{d_o}{d_i\,h_i} + \frac{d_o \ln(d_o/d_i)}{2\,K} + \frac{1}{h_o}} \qquad (22)$$

2.4. The geometric specifications in a shell and tube heat exchanger are as follows:

Table 1 Geometrical Specification

Parameters	**Specification**
Material for tube	Copper
Material for shell	Mild stell
Shell diameter,$\boldsymbol{D_s}$	177.8 mm
Shell wall thickness,$\boldsymbol{t_s}$	6 mm

Tube outer diameter, $\boldsymbol{d_o}$	22.225 mm
Tube inner diameter, $\boldsymbol{d_i}$	19.825 mm
Tube length,l	1500 mm
Tube arrangments	Square
Baffle number,	4
Baffle cut	25%
Baffle spacing,b	360 mm
Pitch factor, $\boldsymbol{P_t}$	27.7 mm
Number of tubes, $\boldsymbol{N_t}$	4
Fouling resistance of tube, $\boldsymbol{R_{f_i}}$	0.00035 m^2 K/W
Fouling resistance of shell, $\boldsymbol{R_{f_o}}$	0.000176 m^2 K/W
Thermal conductivity of copper, $\boldsymbol{K_{copper}}$	385 W/mK

2.5 Statistical and Performance Analysis

Following the calculation of the thermal-hydraulic performance parameters, the experimental data were subjected to descriptive, statistical, and engineering performance analyses to provide a comprehensive evaluation of the investigated baffle configurations. Descriptive statistics, including the mean, standard deviation, minimum, and maximum values, were calculated for the shell-side Nusselt number, tube-side Nusselt number, number of transfer units (NTU), effectiveness, and pressure drop to summarize the experimental data.

To quantify the performance enhancement achieved by the modified baffle configurations, percentage improvement analysis was performed using the single-segmental baffle as the reference configuration. The percentage improvement for each performance parameter was calculated as

$$\text{Percentage Improvement (\%)} = \frac{X_i - X_{\text{ref}}}{X_{\text{ref}}} \times 100 \quad 23$$

where $X_i$represents the average value of the investigated baffle configuration and X_{ref}represents the corresponding average value for the single-segmental baffle.

A two-way analysis of variance (ANOVA) was subsequently performed to evaluate the effects of baffle configuration and inlet temperature on the measured thermal-hydraulic performance parameters, including the shell-side Nusselt number, tube-side Nusselt number, NTU, effectiveness, and pressure drop. Where statistically significant differences were identified, Tukey's honestly significant difference (HSD) multiple-comparison test was employed to determine the specific pairs of baffle configurations responsible for the observed differences. A significance level of $p < 0.05$ was adopted throughout the statistical analysis.

To assess the combined thermal and hydraulic performance of the investigated baffle configurations, the Performance Evaluation Criterion (PEC) was calculated according to

$$PEC = \frac{Nu/Nu_{\text{ref}}}{(\Delta P/\Delta P_{\text{ref}})^{1/3}} \quad 24$$

where $Nu_{\text{ref}}$and ΔP_{ref}denote the shell-side Nusselt number and pressure drop of the reference single-segmental baffle configuration, respectively. A PEC value greater than unity indicates that the thermal enhancement outweighs the associated hydraulic penalty.

The hydraulic performance was further evaluated by calculating the pumping power required to circulate the shell-side fluid using

$$P_{\text{pump}} = \Delta P \times Q \quad 25$$

where $P_{\text{pump}}$is the pumping power (W), $\Delta P$is the measured shell-side pressure drop (Pa), and $Q$is the volumetric flow rate (m^3/s). This parameter provides an engineering assessment of the energy required to overcome hydraulic resistance for each baffle configuration.

All data processing, statistical analyses, and engineering performance calculations were performed using MATLAB R2024a (MathWorks Inc., Natick, MA, USA).

III.Results and Discussion

3.1. Effects of Reynolds number on Nusselt number

Figure 3 illustrates the effect of Reynolds' number on the Nusselt number for different types of segmental baffles in a shell-and-tube heat exchanger at a shell-side flow rate of 10 L/min and at different temperatures of 65°C, 70°C, and 75°C. The results show that the Nusselt number, based on the internal diameter of the tube, reached its highest value with triple segmental baffles, followed by double segmental baffles, while the lowest values were observed with single segmental baffles under the same operating conditions.

Therefore, changing the segmental baffle configuration leads to an increase in the Nusselt number, with the highest values obtained using triple segmental baffles. This behavior is attributed to the influence of the triple segmental baffle arrangement on the shell-side flow.
Furthermore, increasing the Reynolds number of the flow inside the tube also results in an increase in the Nusselt number due to the greater intensity of turbulent flow.
These results are consistent with several previous studies, which reported that increasing the number of Reynolds and improving the segmental baffle design enhance the thermal performance of shell-and-tube heat exchangers [5], [13].

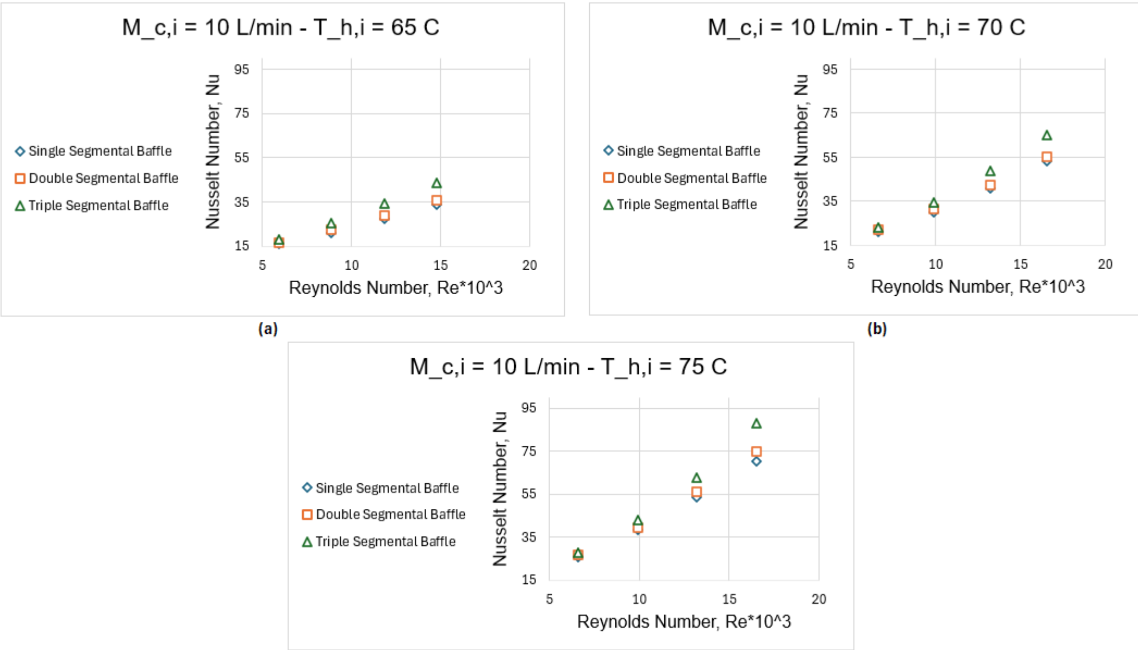

(c)

Figure 2 Effects of the Reynolds number on the Nusselt number of water at different segmental baffles, at mass flow rate of the shell, is 0.1667 Kg/s, and at different temperatures of (a) 65 °C, (b) 70 °C, and (c) 75 °C.

Figure 4 also illustrates the effect of Reynolds number on the Nusselt number at a shell-side flow rate of 15 L/min and at different temperatures of 65°C, 70°C, and 75°C. The results show that the Nusselt number increases with increasing Reynolds number of the fluid flowing inside the tube side due to the greater intensity of turbulent flow.
This increase in the Nusselt number is attributed to the reduction in viscous forces resulting from the increase in fluid temperature, which consequently enhances convective heat transfer, as observed in Figure 3.

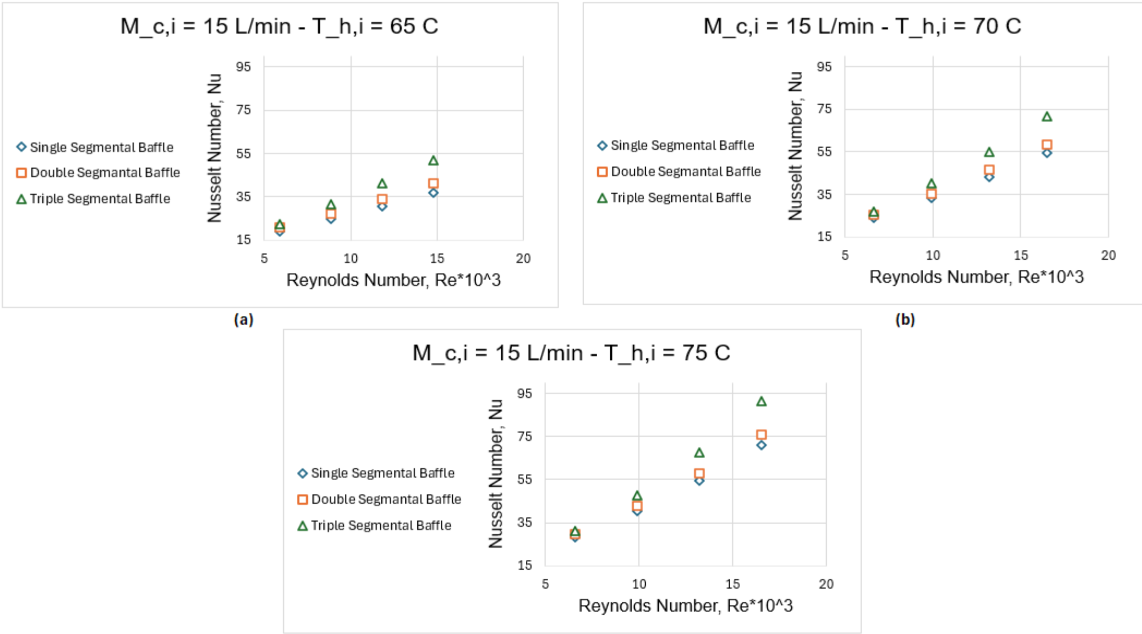

(c)

Figure 3 Effects of the Reynolds number on the Nusselt number of water at different segmental baffles, at mass flow rate of the shell, is 0.25 Kg/s, and at different temperatures of (a) 65 °C, (b) 70 °C, and (c) 75 °C.

Figure 5 further illustrates the effect of Reynolds number on the Nusselt number at a shell-side flow rate of 20 L/min and at different temperatures of 65°C, 70°C, and 75°C. The results show that the Nusselt number increases with increasing Reynolds number of fluid flowing inside the tube-side due to the greater intensity of turbulent flow, which enhances convective heat transfer.
This increase in the Nusselt number is attributed to the reduction in viscous forces resulting from the increase in fluid temperature, which consequently enhances convective heat transfer, as previously discussed.

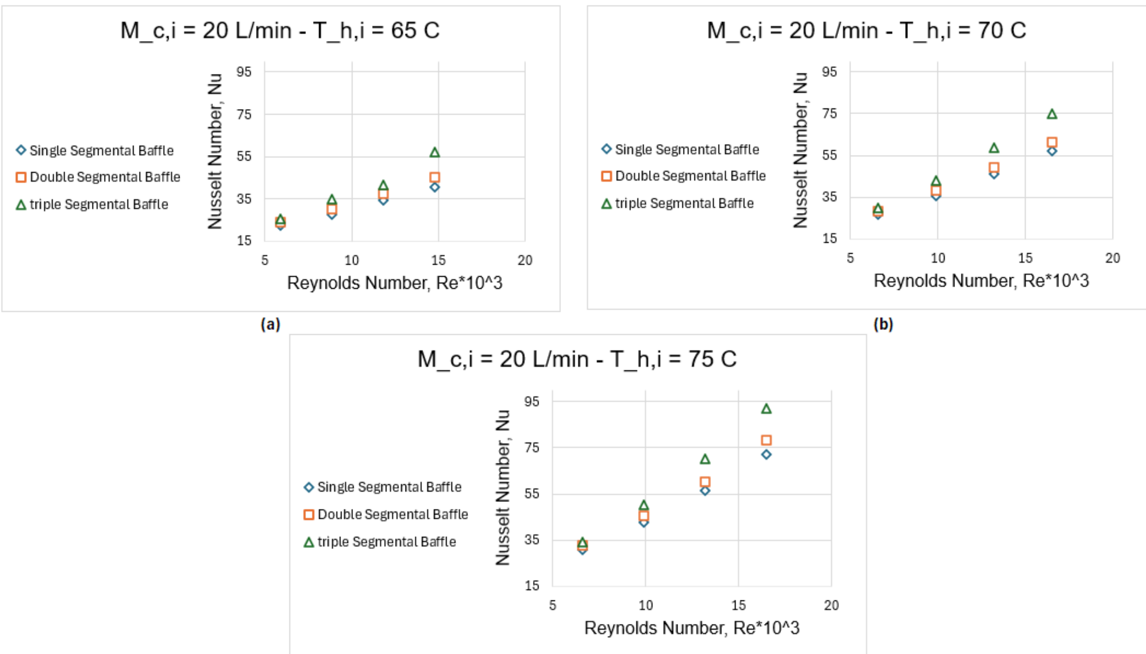

(c)

Figure 4 Effects of the Reynolds number on the Nusselt number of water at different segmental baffles, at mass flow rate of the shell, is 0.3333 Kg/s, and at different temperatures of (a) 65 °C, (b) 70 °C, and (c) 75 °C.

Figure 6 shows the effect of Reynolds' number on the Nusselt number at a shell-side flow rate of 25 L/min and at different temperatures of 65°C, 70°C, and 75°C. The results indicate that the Nusselt number gradually increases with increasing Reynolds number of the fluid flowing inside the tubes due to the increased turbulence intensity and the resulting enhancement in convective heat transfer within the heat exchanger.
This increase in the Nusselt number is attributed to the reduction in viscous forces caused by the rise in fluid temperature, which contributes to enhanced convective heat transfer, as previously explained.

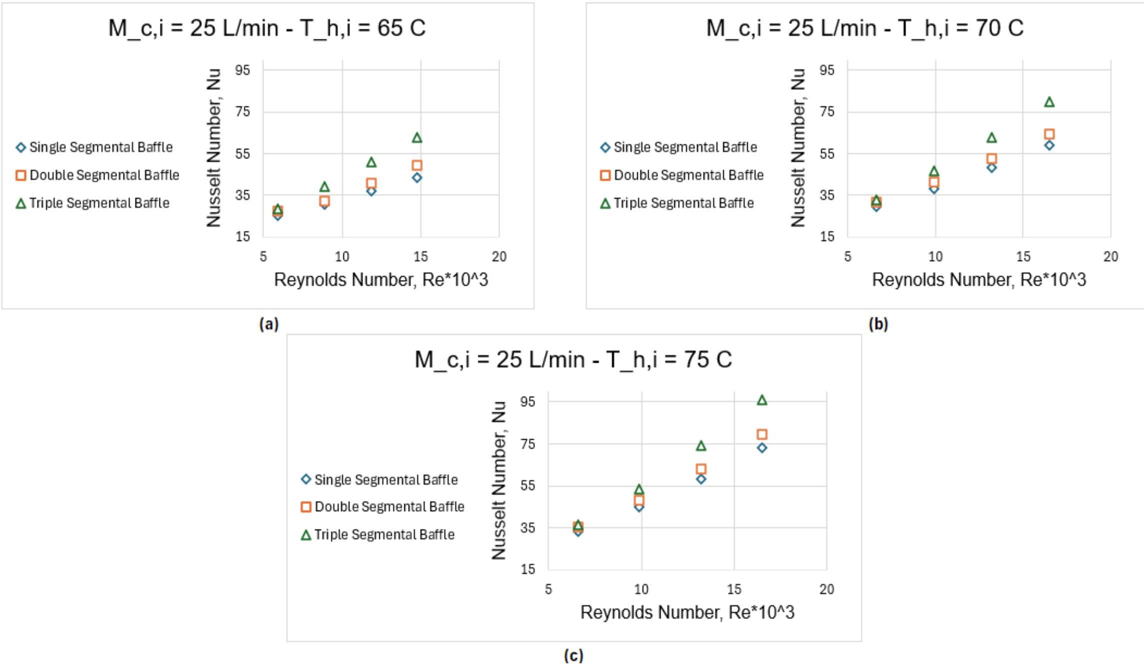

Figure 5 Effects of the Reynolds number on the Nusselt number of water at different segmental baffles, at mass flow rate of the shell, is 0.4167 Kg/s, and at different temperatures of (a) 65 °C, (b) 70 °C, and (c) 75 °C.

Figures 3–6 show that the Nusselt number increases with increasing flow rate within the tubes. This behavior is attributed to the greater intensity of turbulent flow within the heat exchanger, which enhances convective heat transfer. The results also demonstrate that the design of the internal baffles has a significant effect on the Nusselt number. Double-segmental and triple-segmental baffles improve thermal performance compared with single-segmental baffles by promoting better flow distribution and increasing turbulence within the shell side. The highest Nusselt number values were recorded with the triple-segmental baffle configuration.

Percentage Improvement and Statistical Analysis of Nusselt Number

To quantify the thermal enhancement achieved by the modified baffle configurations, the average tube-side Nusselt number was compared with that obtained using the conventional single-segmental baffle. The results showed that the double-segmental baffle increased the average tube-side Nusselt number by 7.27%, whereas the triple-segmental baffle achieved a substantially greater improvement of 24.31% relative to the single-segmental configuration. In contrast, the average shell-side Nusselt number exhibited only marginal improvements of 0.14% and 0.97% for the double- and triple-segmental baffles, respectively.

To determine whether these differences were statistically significant, a two-way analysis of variance (ANOVA) was performed considering baffle configuration and inlet temperature as the independent factors. The results indicated that the baffle configuration had no statistically significant effect on the shell-side Nusselt number ($p = 0.963$), indicating that the observed shell-side improvements were negligible. However, the tube-side Nusselt number was significantly affected by baffle configuration ($p = 0.0075$) as well as inlet temperature ($p < 0.001$). No statistically significant interaction between these two factors was observed ($p = 0.999$), indicating that the influence of the baffle configuration remained consistent over the investigated temperature range.

Tukey's honestly significant difference (HSD) post hoc analysis further demonstrated that the triple-segmental baffle produced a significantly higher tube-side Nusselt number than the conventional single-segmental baffle ($p = 0.017$), whereas the differences between the double- and single-segmental baffles and between the double- and triple-segmental baffles were not statistically significant. These findings confirm that the thermal enhancement observed experimentally is primarily associated with the triple-segmental baffle configuration.

Table 2. Percentage improvement of thermal performance relative to the single-segmental baffle.

Parameter	Double (%)	Triple (%)
Shell-side Nusselt number	0.14	0.97
Tube-side Nusselt number	7.27	24.31
NTU	5.28	16.43
Effectiveness	3.44	10.95
Pressure drop	-19.66	-28.21

3.2. Effects of Reynolds number on the Number of transfer units (NTU).

Figure 7 illustrates the effect of the Reynolds number on the number of heat transfer units (NTU) when using different types of segmental baffles inside a heat exchanger, at a mass flow rate of 10 L/min inside the shell and at different operating temperatures of 65°C, 70°C, and 75°C, respectively. The results show that the NTU value increases with increasing numbers of Reynolds. This is attributed to the increased flow rate inside the tubes, which leads to a higher fluid heat capacity and a lower shell flow rate than the tube flow rate, thus increasing the NTU value.

Furthermore, the design of the internal baffles significantly affects the number of heat transfer units. Double segmental baffles and triple segmental baffles improved thermal performance compared to single segmental baffles due to improved flow distribution and increased turbulence inside the shell. This resulted in a higher heat transfer coefficient and improved heat exchanger efficiency.

It was also observed that higher operating temperatures lead to an increase in the NTU value. This is due to the improved convection heat transfer coefficient inside the tubes with higher fluid temperature and a reduced viscosity effect, which enhances heat transfer efficiency within the heat exchanger.

Furthermore, the minimum heat capacity (C_{min}) in this case represents the heat capacity of the cold shell side ($C_{shell, cold}$). Therefore, changes in the flow rate on this side directly affect the NTU value.

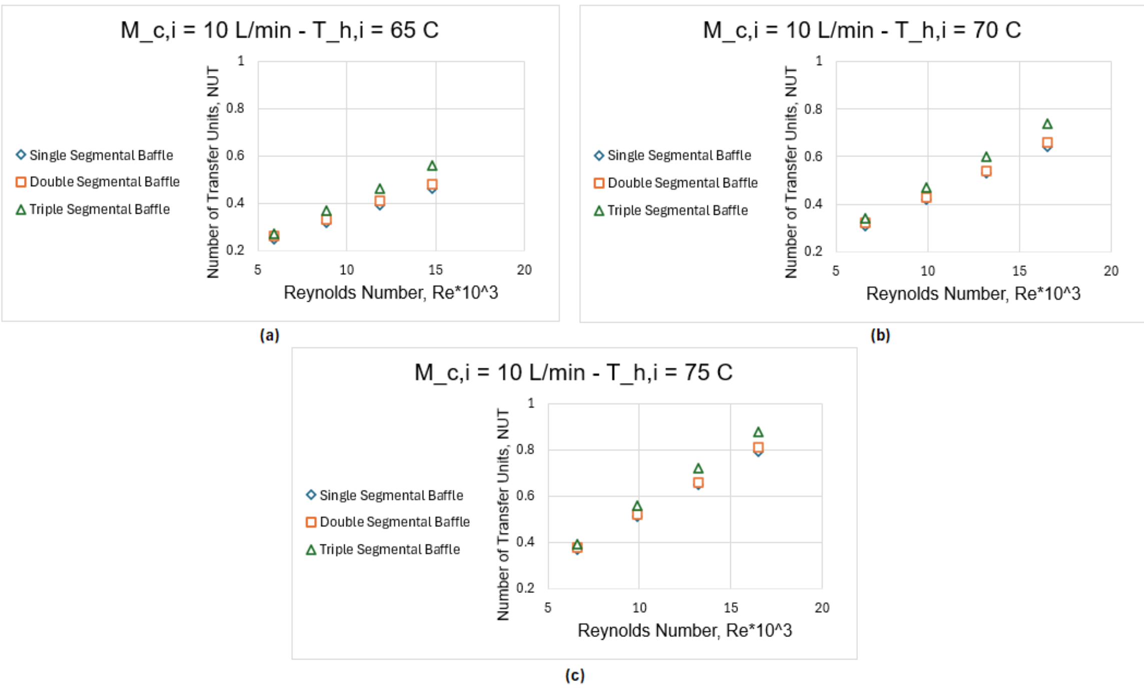

Figure 6 Effects of the Reynolds number on the Number of transfer units (NTU) of water at different segmental baffles, at mass flow rate of the shell, is 0.1667 Kg/s, and at different temperatures of (a) 65 °C, (b) 70 °C, and (c) 75 °C.

Figure 8 illustrates the effect of the Reynolds number on the number of heat transfer units (NTU) when using different types of segmental baffles within a shell-and-tube heat exchanger, at a shell-side flow rate of 15 L/min and at different operating temperatures of 65°C, 70°C, and 75°C, respectively. The results show that the NTU values vary depending on the type of baffles used, due to its effect on the flow pattern and heat transfer efficiency within the shell, also shows that the behavior of the number of heat transfer units (NTU) varies depending on the value of the minimum heat capacity (C_{min}). When ($C_{min} = C_{shell,\ cold}$), the NTU value increases due to the lower heat capacity on the shell side compared to the tube side, thus increasing heat transfer efficiency. Conversely, when ($C_{min} = C_{tube,\ hot}$), the NTU value decreases due to the increased flow rate and heat capacity within the tubes, resulting in an inverse relationship between NTU and C_{min}.

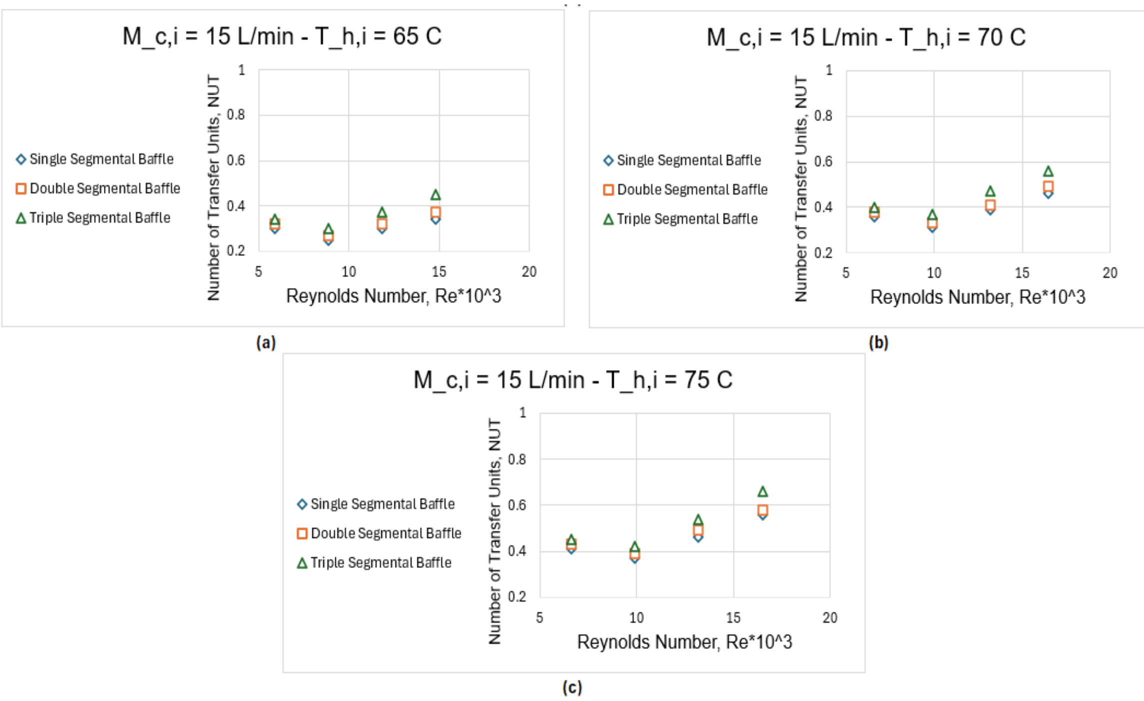

Figure 7 Effects of the Reynolds number on the Number of transfer units (NTU) of water at different segmental baffles, at mass flow rate of the shell, is 0.25 Kg/s, and at different temperatures of (a) 65 °C, (b) 70 °C, and (c) 75 °C.

Figure 9 illustrates the effect of the Reynolds number on the number of heat transfer units (NTU) when using single, double, and triple segmental baffles within a shell-and-tube heat exchanger, at a shell-side flow rate of 20 L/min and at different operating temperatures of 65°C, 70°C, and 75°C, respectively. The results show that the NTU values vary depending on the type of baffles used, due to the baffles' influence on the flow distribution and turbulence within the shell, which directly impacts heat transfer efficiency.

As shown in figure 9, the behavior of the heat transfer units is highly dependent on the minimum heat capacity (C_{min}). In cases where ($C_{min} = C_{shell,\ cold}$), the NTU value increases because of the lower heat capacity on the shell side compared to the tube side, thus enhancing the efficiency of heat transfer within the heat exchanger. However, when the minimum heat capacity is shifted to the side of the tube ($C_{min} = C_{tube,\ hot}$), the NTU value decreases due to the increased flow rate and heat capacity within the tube, resulting in an inverse relationship between NTU and (C_{min}).

ISSN: 2248-9622, Vol. 16, Issue 8, August 2026, pp 35-54

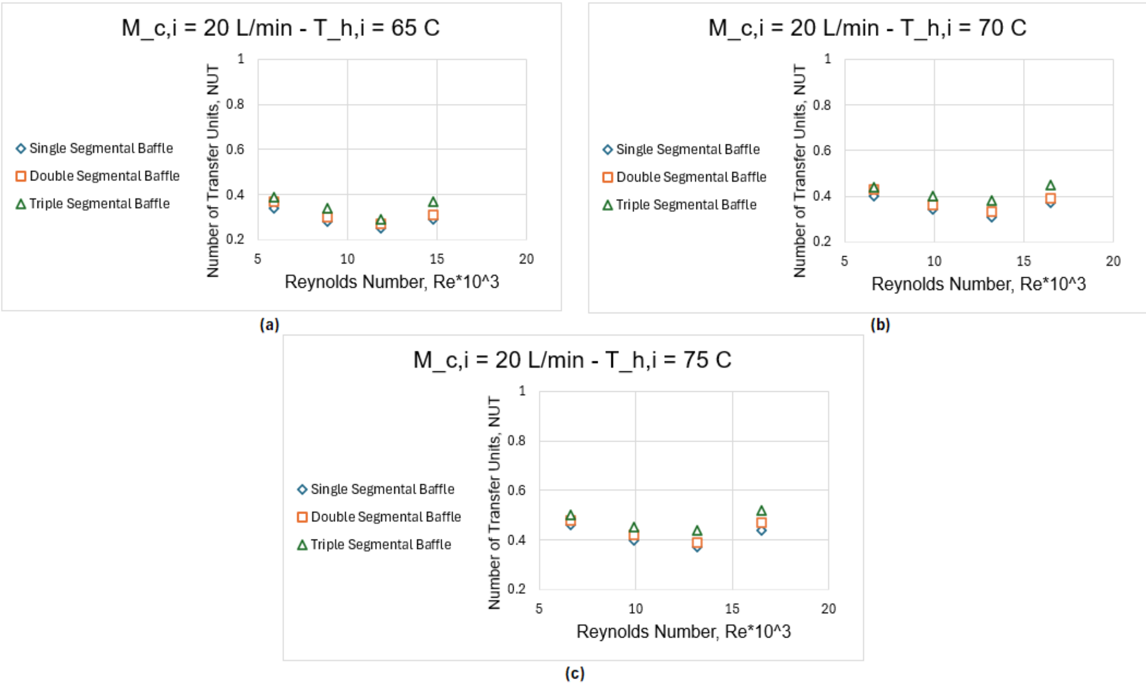

Figure 8 Effects of the Reynolds number on the Number of transfer units (NTU) of water at different segmental baffles, at mass flow rate of the shell, is 0.333 Kg/s, and at different temperatures of (a) 65 °C, (b) 70 °C, and (c) 75 °C.

Figure 10 illustrates the effect of Reynolds' number on the number of transfer units (NTU) for single-, double-, and triple-segmental baffle configurations in a shell-and-tube heat exchanger at a shell-side flow rate of 25 L/min and operating temperatures of 65°C, 70°C, and 75°C. The results show that the NTU values vary depending on the baffle configuration used, due to its influence on flow distribution and turbulence within the shell, which directly affects the heat transfer performance of the heat exchanger. The figure also shows that the NTU values gradually decrease with increasing number of Reynolds for all baffle configurations. This is attributed to the increased flow rate within the tubes, which leads to a higher heat capacity on the tube side. Consequently, the minimum heat capacity (C_{min}) is represented by ($C_{min} = C_{tube, hot}$). Since the relationship between NTU and (C_{min}) is inverse, increasing ($C_{min} = C_{tube, hot}$) results in a decrease in the NTU values as the Reynolds number increases.

It is also noted that the triple segmental baffle achieved relatively higher NTU values compared to the single and double segmental baffles, as a result of its ability to improve flow distribution and increase its turbulence within the shell, which contributed to improving the efficiency of heat transfer and raising the thermal performance of the heat exchanger.

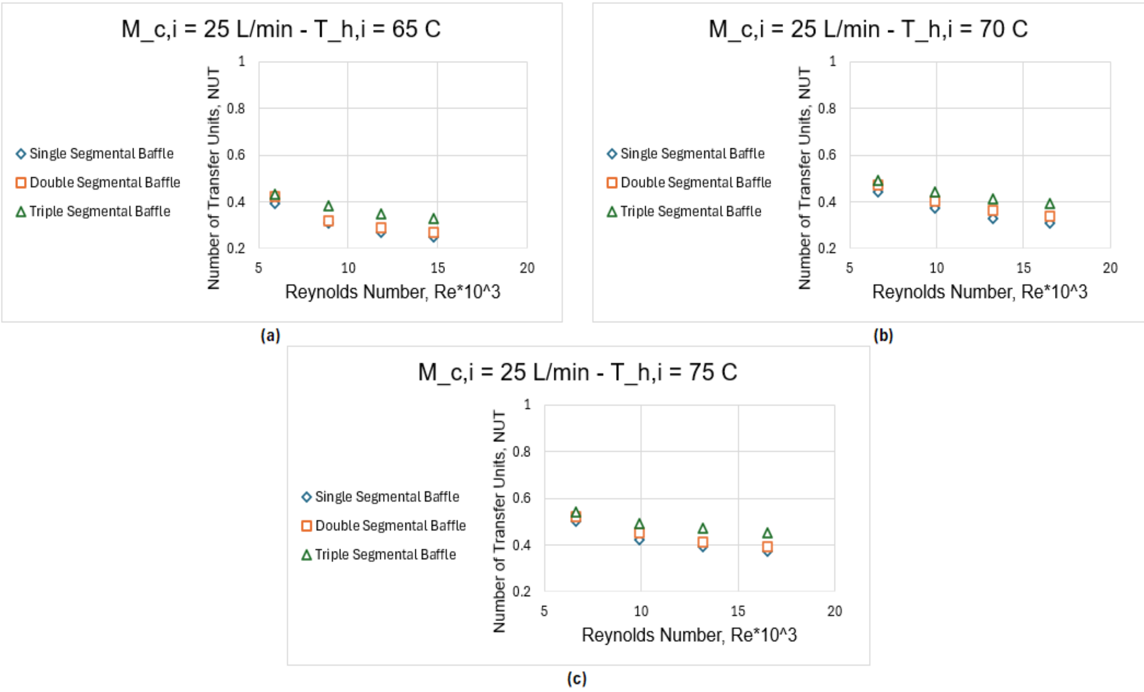

Figure 9 Effects of the Reynolds number on the Number of transfer units (NTU) of water at different segmental baffles, at mass flow rate of the shell, is 0.4167 Kg/s, and at different temperatures of (a) 65 °C, (b) 70 °C, and (c) 75 °C.

Figures (7 – 10) show that the number of heat transfer units (NTU) is directly affected by the number of Reynolds and the type of segmental baffles used within the shell and tube heat exchanger. The results showed that NTU values gradually decrease with increasing Reynolds number when the minimum heat capacity (C_{min}) is equal to the tube side ($C_{min} = C_{tube,\ hot}$). This is due to the increased flow rate and higher heat capacity within the tubes, resulting in an inverse relationship between NTU and (C_{min}). This finding is in agreement with the results reported by Hozaifa et al [13]. Conversely, NTU values tend to increase when the minimum heat capacity (C_{min}) is equal to the shell side ($C_{min} = C_{shell,\ cold}$), because the lower heat capacity on this side enhances heat transfer efficiency, this finding is in agreement with the results reported by [14].

The results also show that the triple-segmental baffle configuration achieved the highest NTU values compared with the other configurations, followed by the double-segmental and single-segmental baffle configurations. This behavior is attributed to the ability of triple-segmental baffles to improve flow distribution and increase turbulence intensity within the shell side, thereby enhancing heat transfer efficiency and improving the thermal performance of the heat exchanger.

Statistical analysis confirmed the experimental observations regarding the thermal performance of the heat exchanger. Two-way ANOVA demonstrated that both the baffle configuration ($p = 0.0045$) and inlet temperature ($p < 0.001$) significantly influenced the number of transfer units (NTU), whereas their interaction was not statistically significant ($p = 1.000$). Furthermore, Tukey's HSD multiple-comparison test revealed that the triple-segmental baffle achieved significantly higher NTU values than the conventional single-segmental configuration ($p = 0.015$), while no statistically significant differences were observed between the double-segmental baffle and the other two configurations. These findings indicate that the improved flow distribution produced by the triple-segmental baffle contributes directly to enhanced overall heat-transfer performance.

3.3. Effects of Reynolds number on Effectiveness (ε).

Figure 11 illustrates the effect of Reynolds number on the effectiveness of a shell-and-tube heat exchanger using single-, double-, and triple-segmental baffle configurations at a tube-side flow rate of 10 L/min and operating temperatures of 65°C, 70°C, and 75°C. Effectiveness is defined as the ratio of the actual heat transfer rate (Q_{actual}) to the maximum heat transfer rate, where the maximum heat transfer rate (Q_{max}) depends directly on the minimum heat capacity (C_{min}), as stated in Equation 3.20.

The results in this figure show that effectiveness increases with increasing Reynolds number. This is

because the minimum heat capacity (C_{min}) in this case is equal to the shell side ($C_{min} = C_{shell,\ cold}$).
The design of segmental baffles also has a significant influence on heat exchanger effectiveness. The triple-segmental baffle configuration achieved the highest effectiveness values, followed by the double-segmental and single-segmental baffle configurations. This behavior is attributed to the superior ability of triple-segmental baffles to improve flow distribution and increase turbulence within the shell side, thereby enhancing the thermal performance of the heat exchanger.

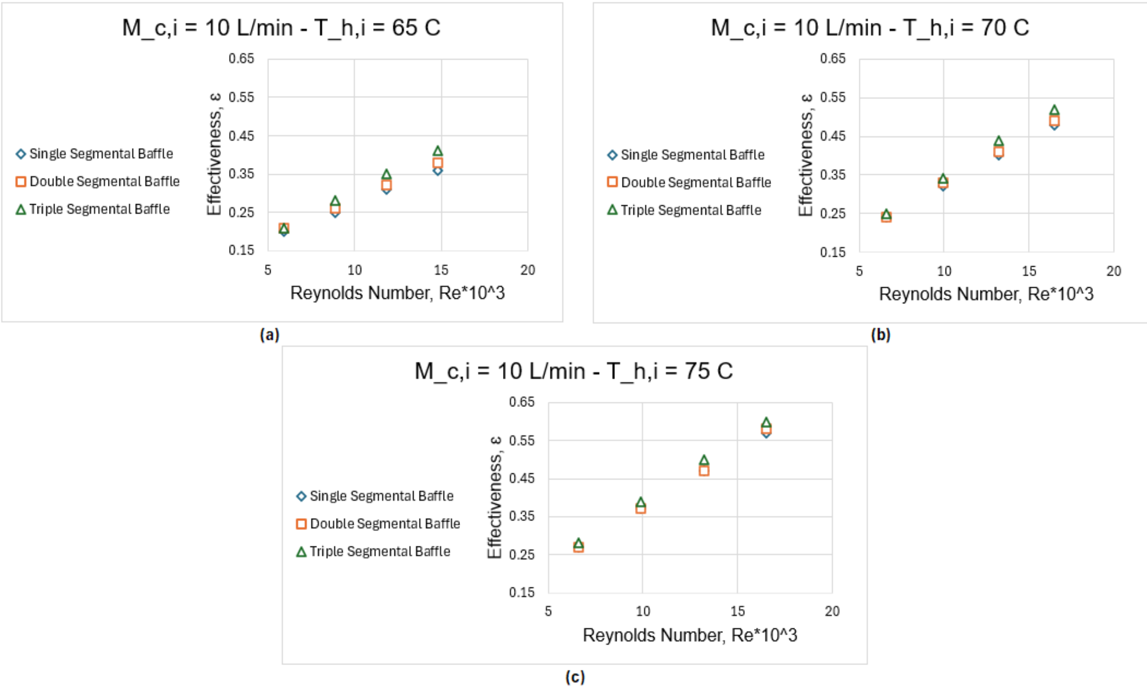

Figure 10 Effects of the Reynolds number on the Effectiveness (ε) of water at different segmental baffles, at mass flow rate of the shell, is 0.1667 Kg/s, and at different temperatures of (a) 65 °C, (b) 70 °C, and (c) 75 °C.

Figure 12 illustrates the effect of the Reynolds number on effectiveness when using single, double, and triple segmental baffles within a shell and tube heat exchanger, at a tube flow rate of 15 L/min and at different operating temperatures of 65°C, 70°C, and 75°C, respectively.

The results show that the effectiveness of behavior varies depending on the value of (C_{min}). When ($C_{min} = C_{shell,\ cold}$), the effectiveness increases with increasing Reynolds number due to improved heat transfer and higher turbulent flow intensity within the shell. Conversely, when ($C_{min} = C_{tube,\ hot}$), the effectiveness values begin to decrease with increasing Reynolds number due to increased tube heat capacity and higher heat transfer rate, resulting in an inverse relationship between the effectiveness and (C_{min}).

It was also observed that the design of the internal baffles has a significant effect on effectiveness, with the triple-segmental baffle configuration achieving the highest effectiveness values, followed by the double-segmental and single-segmental baffle configurations. This behavior is attributed to the superior ability of triple-segmental baffles to improve flow distribution and increase turbulence within the shell side, thereby enhancing the thermal performance of the heat exchanger.

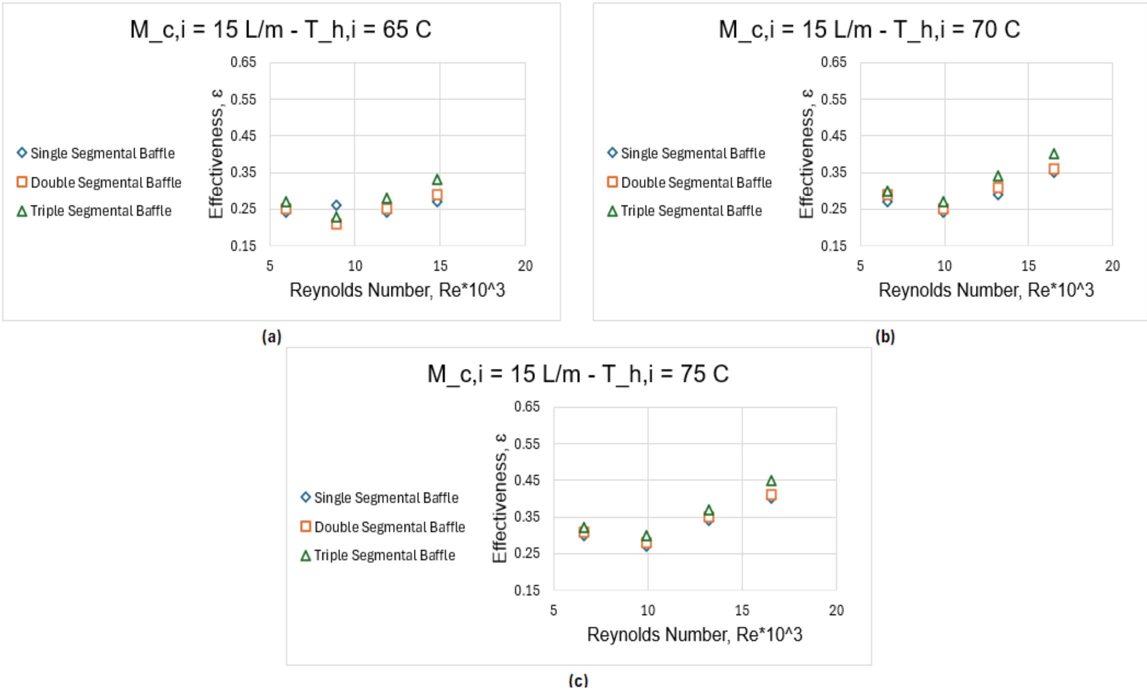

Figure 11 Effects of the Reynolds number on the Effectiveness (ε) of water at different segmental baffles, at mass flow rate of the shell, is 0.25 Kg/s, and at different temperatures of (a) 65 °C, (b) 70 °C, and (c) 75 °C.

Figure 13 illustrates the effect of Reynolds number on the effectiveness of a shell-and-tube heat exchanger using single-, double-, and triple-segmental baffle configurations at a tube-side flow rate of 20 L/min and operating temperatures of 65°C, 70°C, and 75°C.

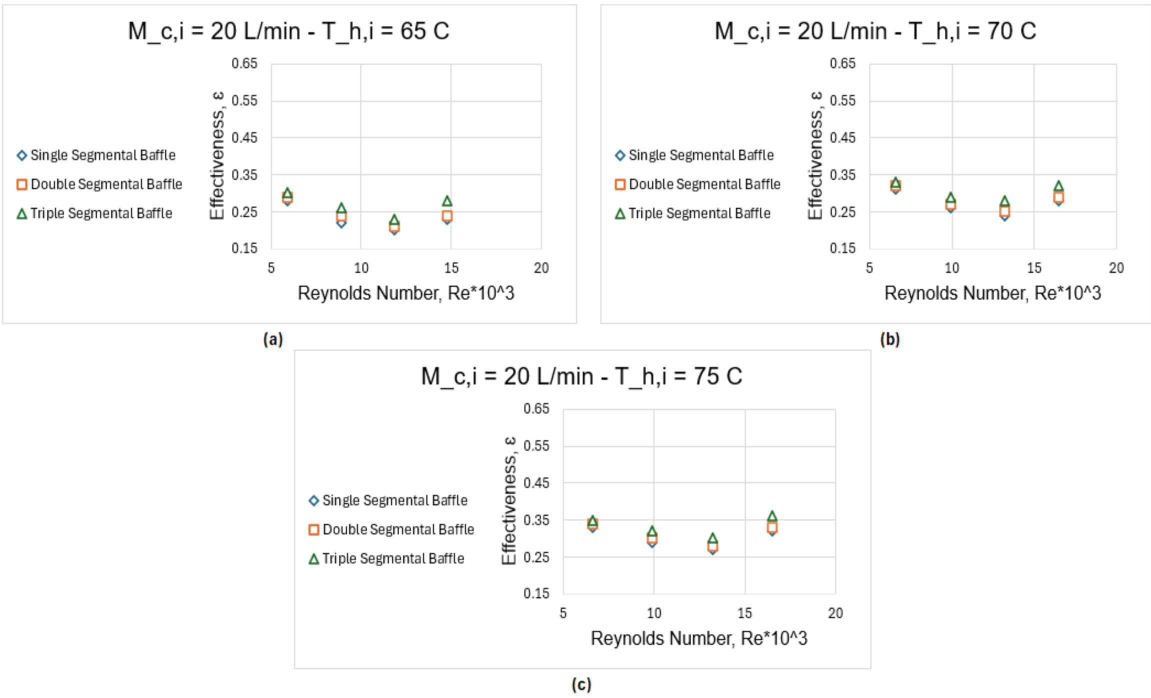

Figure 12 Effects of the Reynolds number on the Effectiveness (ε) of water at different segmental baffles, at mass flow rate of the shell, is 0.25 Kg/s, and at different temperatures of (a) 65 °C, (b) 70 °C, and (c) 75 °C.

Figure 14 illustrates the effect of the Reynolds number on effectiveness when using single, double, and triple segmental baffles within a shell and tube heat exchanger, at a tube flow rate of 25 L/min and

operating temperatures of 65, 70, and 75 °C, respectively.
The results show that the effectiveness decreases gradually with increasing Reynolds number. This is because the minimum heat capacity (C_{min}) in this case is the tube side ($C_{min} = C_{tube,\ hot}$). Increasing the tube flow rate leads to a higher Cmin and a higher maximum heat transfer rate, resulting in lower effectiveness values due to the inverse relationship between them and (C_{min}).

The results also show that the type of segmental baffle used has a significant effect on effectiveness. The triple-segmental baffle configuration exhibited the highest effectiveness values, followed by the double-segmental and single-segmental baffle configurations. This behavior is attributed to the ability of triple-segmental baffles to improve the flow pattern and increase turbulence intensity within the shell side, resulting in enhanced heat transfer efficiency and improved thermal performance of the heat exchanger.

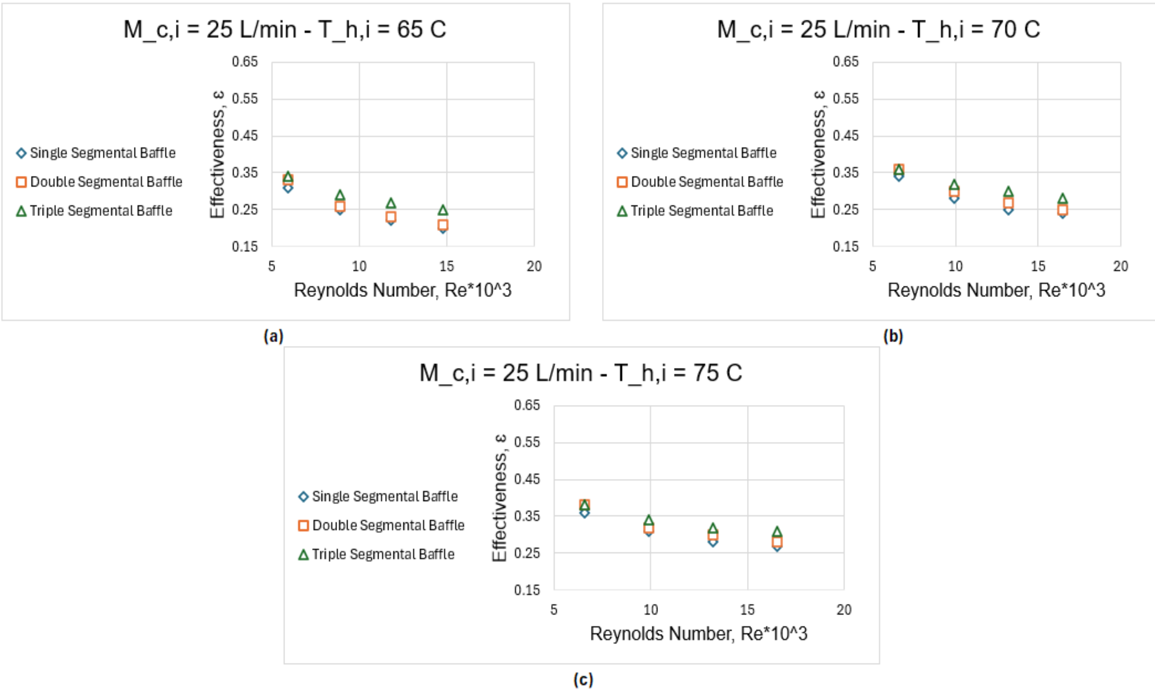

Figure 13 Effects of the Reynolds number on the Effectiveness (ε) of water at different segmental baffles, at mass flow rate of the shell, is 0.4167 Kg/s, and at different temperatures of (a) 65 °C, (b) 70 °C, and (c) 75 °C.

Figures 11 – 14 demonstrate that the effectiveness is directly affected by the number of Reynolds baffles and the type of segmental baffles used within the heat exchanger. The results show that the effectiveness value gradually decreases with increasing Reynolds number when the minimum heat capacity (C_{min}) is located on the tube side ($C_{min} = C_{tube,\ hot}$). This is due to the increased flow rate and higher heat capacity within the tubes, leading to a higher maximum heat transfer rate and an inverse relationship between effectiveness and (C_{min}). This finding is in agreement with the results reported by [15], [16]. Conversely, effectiveness tends to increase when the minimum heat capacity (C_{min}) is located on the cold shell side ($C_{min} = C_{shell,\ cold}$). This is because the lower heat capacity on this side enhances heat transfer efficiency within the heat exchanger, this finding is in agreement with the results reported by [14].
Furthermore, the results show that triple segmental baffles achieved the highest effectiveness values compared to double and then single segmental baffles. This is attributed to the triple segmental baffles' ability to improve flow distribution and significantly increase turbulence within the shell, thus enhancing heat transfer and improving the overall thermal performance of the heat exchanger.

3.4. Effects of Reynolds number on the pressure drops.
Figure 15 illustrates a comparison of the shell-side pressure drop for single-, double- and triple-segmental baffle configurations at flow rates ranging from 10 to 25 L/min. The results show that the triple-segmental baffle configuration exhibited the lowest pressure drop throughout the investigated flow rate range, followed by the double-segmental baffle configuration, while the single-segmental baffle configuration recorded the highest pressure drop.
The results indicate that the pressure drop is not solely dependent on the number of baffles but is also

strongly influenced by the flow distribution within the shell. The triple-segmental baffle configuration improved the flow path and reduced bypass flow and stagnant regions, which are major sources of hydraulic losses.

In addition, the more uniform flow distribution provided by the triple-segmental baffle configuration reduced the occurrence of high local velocities caused by sharp flow turns or localized flow concentrations. These conditions are often associated with increased frictional losses in simpler baffle configurations. As a result, the flow became more stable within the shell, leading to a lower overall pressure drop.

Furthermore, the triple-segmental baffle arrangement reduced the length of undirected flow paths, thereby minimizing variations in velocity distribution within the shell. This suggests that the geometric design of the baffles may have a greater influence on hydraulic performance than merely increasing their number.

These results highlight the importance of considering baffles not only as turbulence-promoting elements but also as effective means of controlling flow distribution and reducing unnecessary hydraulic losses. Therefore, the improved hydraulic performance achieved by the triple-segmental baffle configuration in this study demonstrates the significant role of internal geometry in attaining better flow regulation.

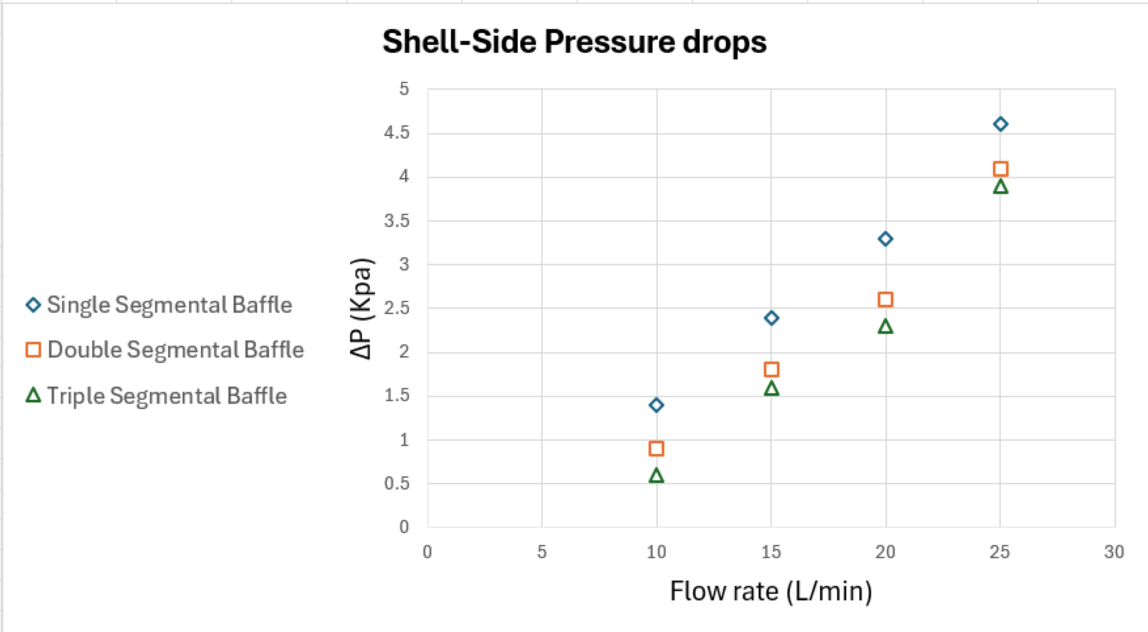

Figure 14 Effects of the Reynolds number on the pressure drops at different segmental baffles.

Figure 16 illustrates the effect of flow rate on pressure drop on the tube side of the heat exchanger. The results show that the pressure drop increases with increasing flow rate due to the higher water velocity within the tubes.

Furthermore, the pressure drop is not limited to the flow inside the tubes themselves but also includes the water collection and distribution regions located at the tube inlets and outlets (headers). In these regions, the fluid experiences change in both direction and velocity before entering and after exiting the tubes, resulting in additional pressure losses on the tube side of the heat exchanger.

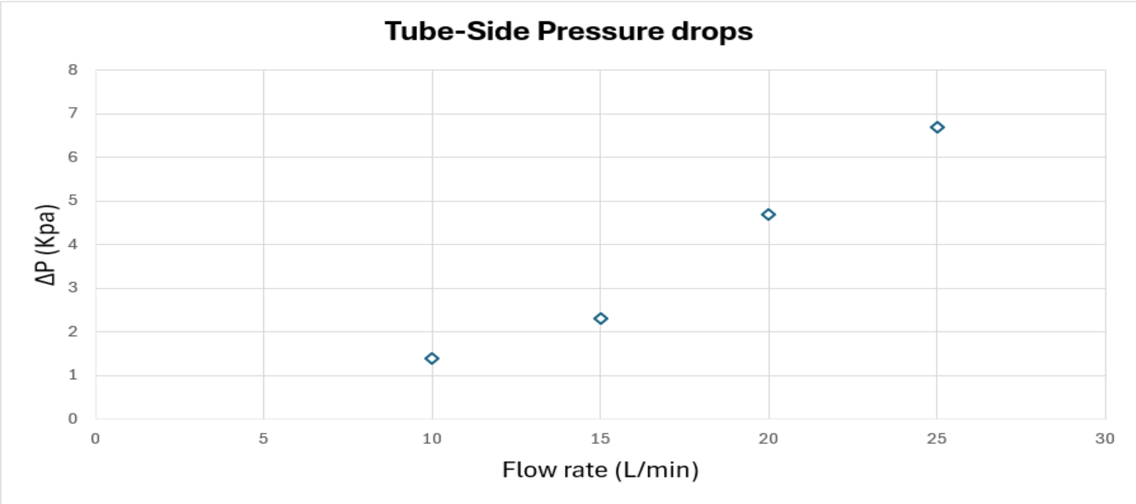

Figure 15 Effects of the Reynolds number on pressure drops.

The pressure drops presented in Figures 15 and 16 for both the shell and tube sides of the heat exchanger show that pressure drop values increase with increasing flow rate due to the higher flow velocity within the heat exchanger. The results also indicate that the shell-side pressure drop is significantly influenced by the design of the segmental baffles, which modifies the flow path and increases turbulence. In contrast, the pressure drop on the tube side is primarily associated with the fluid flow velocity within the tubes, in addition to the losses occurring at the water collection and distribution regions located at the tube inlets and outlets.

Hydraulic Performance Evaluation

In addition to reducing the pressure drop, the modified baffle configurations substantially improved the hydraulic performance of the heat exchanger. Relative to the conventional single-segmental baffle, the average shell-side pressure drop decreased by 19.66% for the double-segmental configuration and by 28.21% for the triple-segmental configuration. Statistical evaluation confirmed that the influence of baffle configuration on pressure drop was significant ($p = 0.0041$), whereas inlet temperature exhibited no statistically significant effect ($p = 1.000$). Tukey's HSD analysis further demonstrated that both the double-segmental ($p = 0.049$) and triple-segmental ($p = 0.002$) baffles produced significantly lower pressure drops than the conventional single-segmental configuration. However, no statistically significant difference was observed between the double- and triple-segmental configurations.

The reduction in pressure loss was also reflected in the required pumping power. The average pumping power decreased from 0.963 W for the single-segmental configuration to 0.794 W and 0.723 W for the double- and triple-segmental configurations, corresponding to reductions of approximately 17.5% and 24.9%, respectively. These reductions indicate that the modified baffle arrangements reduce hydraulic resistance while simultaneously maintaining or improving thermal performance, thereby lowering the energy required to operate the heat exchanger.

Table 3. Hydraulic performance comparison of the investigated baffle configurations.

Configuration	Pressure Drop (kPa)	Pumping Power (W)
Single	2.925	0.963
Double	2.350	0.794
Triple	2.100	0.723

3.5 Overall Thermal–Hydraulic Performance Assessment

The overall thermal–hydraulic performance of the investigated baffle configurations was evaluated using the Performance Evaluation Criterion (PEC), which considers both heat-transfer enhancement and hydraulic losses. A PEC value greater than unity indicates that the thermal enhancement outweighs the additional hydraulic penalty associated with the modified configuration.

The calculated PEC values were 1.000, 1.077, and 1.128 for the single-, double-, and triple-segmental baffles, respectively. Both modified configurations therefore outperformed the conventional single-segmental baffle, while the triple-segmental baffle achieved the highest overall thermal–hydraulic performance. These findings demonstrate that the triple-segmental arrangement provides the most favourable balance between enhanced heat transfer and reduced hydraulic resistance among the investigated designs.

Table 4. Performance Evaluation Criterion (PEC).

Configuration	PEC
Single	1.000
Double	1.077
Triple	1.128

IV. Conclusions

This study experimentally evaluated the influence of single-, double-, and triple-segmental baffle configurations on the thermal and hydraulic performance of a shell-and-tube heat exchanger under different operating conditions. The results demonstrated that increasing Reynolds number enhanced heat transfer for all investigated configurations, while the triple-segmental baffle consistently exhibited the best overall performance. Compared with the conventional single-segmental baffle, the triple-segmental configuration increased the average tube-side Nusselt number by 24.31%, NTU by 16.43%, and heat exchanger effectiveness by 10.95%, while reducing the shell-side pressure drop by 28.21%. The double-segmental baffle also improved thermal performance, although to a lesser extent.

Statistical analysis confirmed that baffle configuration had a significant effect on the tube-side Nusselt number, NTU, and pressure drop, while inlet temperature significantly influenced the thermal performance parameters. Tukey's HSD analysis further demonstrated that the triple-segmental baffle achieved significantly higher tube-side Nusselt number and NTU values, together with significantly lower pressure drop, than the conventional single-segmental configuration, confirming its superior thermal-hydraulic performance.

The hydraulic assessment further showed that the triple-segmental baffle reduced the average pumping power by approximately 24.9% compared with the single-segmental configuration. Moreover, the Performance Evaluation Criterion (PEC) reached 1.128, exceeding the values obtained for the single- (1.000) and double-segmental (1.077) baffles. These findings demonstrate that the triple-segmental baffle provides the most favourable balance between heat transfer enhancement and hydraulic losses, making it the preferred configuration among those investigated for improving the energy efficiency of shell-and-tube heat exchangers.

Future studies should investigate the influence of baffle spacing, baffle cut ratio, alternative baffle geometries, and advanced working fluids such as nanofluids under a broader range of operating conditions to further optimize the thermal-hydraulic performance of shell-and-tube heat exchangers.

References

[1] R. Zahedi and A. Ahmadi, ‘A comprehensive review of the performance and principle of fluidized bed heat exchangers with solar energy as thermal source’, *Energy Reports*, vol. 13, pp. 4800–4812, Jun. 2025, doi: 10.1016/j.egyr.2025.04.038.

[2] J. K. Adebayo, A. A. Dare, and M. O. Petinrin, ‘Performance characteristics of shell and tube heat exchanger using sectoral baffle’, *J. Eng. Appl. Sci.*, vol. 72, no. 1, p. 13, Jan. 2025, doi: 10.1186/s44147-024-00555-y.

[3] A. M. Mohammadzadeh, B. Jafari, K. Hosseinzadeh, and E. Paikar, ‘Numerical investigation of segmental baffle design in shell and tube heat exchangers with varying inclination angles and spacing’, *Sci Rep*, vol. 15, no. 1, p. 4683, Feb. 2025, doi: 10.1038/s41598-025-87652-x.

[4] M. S. Abdollahpour, M. Fazli, A. Khademi, S. A. A. Mehrjardi, K. Mazaheri, and M. B. Shafii, ‘A critical review of turbulator effects on shell-and-tube heat exchanger performance based on CFD studies’, *International Communications in Heat and Mass Transfer*, vol. 172, p. 110273, Mar. 2026, doi: 10.1016/j.icheatmasstransfer.2025.110273.

[5] S. M. Hasan, S. Iqbal, I. Khan, A. Javaid, and M. Sajid, ‘Performance enhancement of a shell-and-tube heat exchanger using a novel baffle design’, *Case Studies in Thermal Engineering*, vol. 74, p. 106800, Oct. 2025, doi: 10.1016/j.csite.2025.106800.

[6] A. M. Mohammadzadeh, B. Jafari, and K. Hosseinzadeh, ‘Comprehensive numerical investigation of the effect of various baffle design and baffle spacing on a shell and tube heat exchanger’, *Applied Thermal Engineering*, vol. 249, p. 123305, Jul. 2024, doi: 10.1016/j.applthermaleng.2024.123305.

[7] A. S. Ambekar, R. Sivakumar, N. Anantharaman, and M. Vivekenandan, ‘CFD simulation study of shell and tube heat exchangers with different baffle segment configurations’, *Applied Thermal Engineering*, vol. 108, pp. 999–1007, Sep. 2016, doi: 10.1016/j.applthermaleng.2016.08.013.

[8] M. A. Hossain, M. Mamun, M. K. Islam, Al-Amin, M. O. Faruk, and S. Hossen, 'Experimental Study on The Influence of Baffles on Heat Transfer of Shell and Tube Heat Exchanger', *SciEn Conference Series: Engineering*, vol. 3, pp. 353–358, Nov. 2025, doi: 10.38032/scse.2025.3.99.

[9] R. Kumar and M. Pandey, 'Heat transfer enhancement and pressure drop characteristics of miniature channels with microfins of axially varying pitch', *International Communications in Heat and Mass Transfer*, vol. 166, p. 109200, Aug. 2025, doi: 10.1016/j.icheatmasstransfer.2025.109200.

[10] A. Vafadar, F. Guzzomi, and K. Hayward, 'Experimental Investigation and Comparison of the Thermal Performance of Additively and Conventionally Manufactured Heat Exchangers', *Metals*, vol. 11, no. 4, p. 574, Apr. 2021, doi: 10.3390/met11040574.

[11] S. Kakaç, H. Liu, and A. Pramuanjaroenkij, *Heat Exchangers: Selection, Rating, and Thermal Design, Fourth Edition*, 4th edn. Boca Raton: CRC Press, 2020. doi: 10.1201/9780429469862.

[12] F. P. Incropera, T. L. Bergman, A. S. Lavine, and D. P. Dewitt, *Fundamentals of Heat and Mass Transfer*, 7th Edition. John Wiley & Sons, 2011.

[13] C. Nie, Z. Chen, X. Liu, H. Li, J. Liu, and Z. Rao, 'Design of metal foam baffle to enhance the thermal-hydraulic performance of shell and tube heat exchanger', *International Communications in Heat and Mass Transfer*, vol. 159, p. 108005, Dec. 2024, doi: 10.1016/j.icheatmasstransfer.2024.108005.

[14] V. N. Rao and B. R. Sankar, 'Heat transfer and friction factor investigations of CuO nanofluid flow in a double pipe U-bend heat exchanger', *Materials Today: Proceedings*, vol. 18, pp. 207–218, Jan. 2019, doi: 10.1016/j.matpr.2019.06.294.

[15] T. Han, Q. Li, L. Shang, X. Chen, F. Zhou, and W. Li, 'Study on the Influence of Reynolds Number on Heat Exchange Performance and Nusselt Number of Spray Coil Heat Exchanger', *Processes*, vol. 13, no. 2, p. 588, Feb. 2025, doi: 10.3390/pr13020588.

[16] M. B. Slimene, S. Poncet, J. Bessrour, and F. Kallel, 'Numerical investigation of the flow dynamics and heat transfer in a rectangular shell-and-tube heat exchanger', *Case Studies in Thermal Engineering*, vol. 32, p. 101873, Apr. 2022, doi: 10.1016/j.csite.2022.101873.

Nomenclature

Symbol	**Definition**
A_i	The surface area of inner tube
A_s	Bundle crossflow area
A_{tp}	Total area of tube
C_p	specific heat
D_e	Equivalent diameter
D_s	Shell diameter
G_s	Shell-side mass velocity
N_t	Number of tubes
P_T	Tube Pitch
P_r	Prantl number
Q_{avg}	heat transfer rate average
R_{f_i}	fouling resistance of tube
R_{f_o}	fouling resistance of shell
T_b	Bulk Temperature
U_c	overall heat transfer coefficient without fouling
U_f	overall heat transfer coefficient with considering fouling
d_i	Tube inner diameter
d_o	Tube outer diameter
$\dot{m}$	Mass flow rate
u_m	Tube velocity
ΔT_{LM}	logarithmic mean temperature difference
B	Baffle spacing
C	The clearance
F	Fraction Factor
h	Heat transfer coefficient
K	Thermal conductivity
L	Length
Nu	Nusselt number
Re	Reynolds number
T	Temperature
t	Thickness
NUT	number of transfer units
Q	heat transfer rate
PEC	Performance Evaluation Criterion
P_{pump}	Hydraulic pumping power

Subscripts

avg	Average
c	Cold
h	Hot
i	Inner
In	Inner surface of the tube
max	Maximum
min	Minimum
o	Outer
out	Outer surface of the tube
S	Shell-side
t	Tube-side
W	Wall